Theoretical Study on the Kinetics of the Reaction CH2Br + NO2

ARTICLE *in* THE JOURNAL OF PHYSICAL CHEMISTRY A · APRIL 2014

Impact Factor: 2.69 · DOI: 10.1021/jp410811m · Source: PubMed

THE JOURNAL OF PHYSICAL CHEMISTRY A

Article

pubs.acs.org/JPCA

Theoretical Study on the Kinetics of the Reaction $CH_2Br + NO_2$

Lei Yang,[†,‡] Jing-Yao Liu,*[,†] Cheng Luo,[†] and John R. Barker[‡]

[†]Institute of Theoretical Chemistry, State Key Laboratory of Theoretical and Computational Chemistry, Jilin University, Changchun 130023, People's Republic of China

[‡]Atmospheric, Oceanic, and Space Sciences, University of Michigan, Ann Arbor, Michigan 48109-2143, United States

Supporting Information

ABSTRACT: The mechanism for the reaction $CH_2Br + NO_2$ was investigated by quantum chemical calculation, and the kinetic calculations were carried out by means of multichannel RRKM and variational transition-state theory method. Both singlet and triplet potential energy surfaces (PESs) were considered at the CCSD(T)/6-311++G(d,p)//B3LYP/6-311G(d,p) level. The results show that the singlet PES is preferred, and the initial association is a barrierless process ($CH_2Br + NO_2 \rightarrow CH_2BrNO_2$), consistent with previous study, while the reaction occurring on the triplet PES is unfavorable due to the high barriers at the entrance channels. The calculated overall rate constants agree well with the experimental data within the measured temperature range of 221−363 K, fitted to the expression of $k(T) = 2.61 \times 10^{-10} T^{-0.76} \exp(461/T)$ cm^3 molecule^{-1} s^{-1} over the temperature range of 200−2000 K. The product ratios were obtained by using master equation modeling and show that the formation of product CH_2O + BrNO (P1) is dominant, in line with the experimental observation.

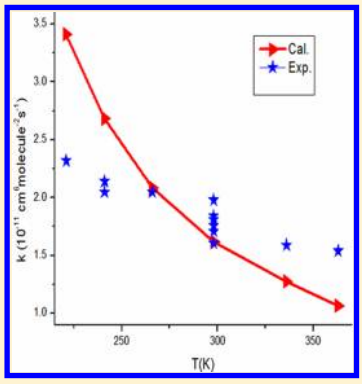

1. INTRODUCTION

Nitrogen dioxide (NO_2) is one of the major atmospheric pollutants released from industrial and automotive exhausts that plays an important role in photochemical smog and the formation of acid rain precursors and has adverse impacts on humans. Carbon-centered free radicals are common intermediates produced in many combustion environments, and the reactions of carbon-centered free radicals with NOx are known to have large rate constants, with high exothermicity. Hence, the detailed information on the kinetics and reactivity of nitrogen oxides toward those radicals is very important for the modeling of NO_2 reducing in combustion processes.[1]

As one of the carbon-centered free radicals, the bromine-substituted methyl radical has received much attention due to the adverse impact of bromine on the atmosphere.[2−4] Recently, the kinetics of the reaction $CH_2Br + NO_2$ have been examined experimentally by Eskola et al. using laser photolysis/photoionization mass spectrometry.[4] In their paper, the decay of radical concentrations was monitored in time-resolved measurements to obtain reaction rate constants under pseudo-first-order conditions, and the bimolecular rate constants of this reaction are very rapid and obey the following temperature dependence: $k(CH_2Br + NO_2) = (1.76 \pm 0.03) \times 10^{-11}(T/300\ \text{K})^{-0.86\pm0.09}$ cm^3 molecule^{-1} s^{-1} (221−363 K). CH_2O and NO were detected as the dominant products of this reaction. Later, Pan et al.[5] investigated both singlet and triplet potential energy surfaces (PESs) for this reaction. The results indicate that the title reaction is more favorable on the singlet PES, and CH_2O is the major product, in line with the experimental observation. However, no kinetic study has been reported to date. Moreover, there is lack of kinetic data in the wide range of temperatures except 221−363 K for the title reaction, which is also relevant to combustion chemistry. Therefore, in the present work, we have investigated the kinetics and mechanism of the reaction by performing quantum chemistry calculations and master equation modeling. Because the barrierless association process is crucial for the rate constant calculations, the relaxed scan for the bond dissociation of intermediate CH_2BrNO_2 was carried out to determine the loose transition state at the entrance channel. Subsequently, on the basis of the energy information on the intermediates and products, which are similar to that in the previous paper,[5] the rate constants and product branching ratios were obtained by variational transition-state theory (VTST) and Rice−Ramsperger−Kassell−Marcus (RRKM) theory over a wide temperature range of 200−2000 K and a pressure range of 2.5−100 Torr. The comparison between theoretical and experimental results was made.

2. COMPUTATIONAL METHODS

In the present work, ab initio calculations were carried out using GAUSSIAN03.[6] Initially, the optimized geometries of the reactants, products, intermediates, and transition states were obtained using the B3LYP method (Beck's three-parameter nonlocal-exchange functional with the nonlocal correlation furnctional of Lee, Yang, and Parr)[7,8] in conjunction with the 6-311G(d,p) basis set. The stationary points were characterized as minima (all real frequencies) or a transition state (one imaginary frequency) by harmonic vibrational frequency

Received: November 2, 2013
Revised: April 13, 2014
Published: April 14, 2014

   dx.doi.org/10.1021/jp410811m | J. Phys. Chem. A 2014, 118, 3313−3318

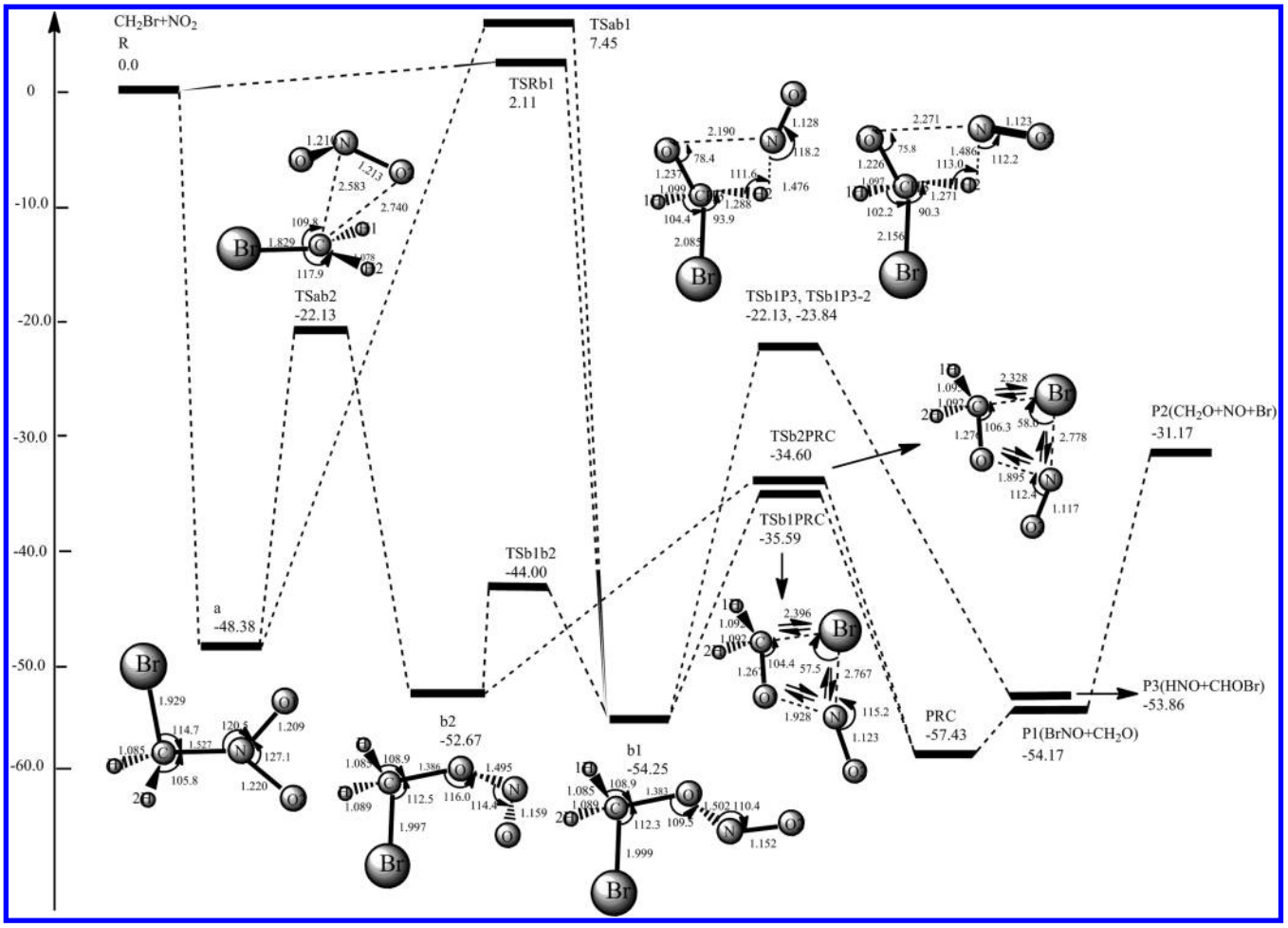

Figure 1. Simplified schematic singlet PES of the relevant reaction pathways for the $CH_2Br + NO_2$ reaction. Relative energies (kcal/mol) are calculated at the CCSD(T)/6-311++G(d,p)//B3LYP/6-311G(d,p) + ZPE level.

calculations. The transition states between designated local minima were confirmed by intrinsic reaction coordinate (IRC) calculations at the same level of theory. The single-point energy calculations were performed at the CCSD(T)/6-311++G(d,p) level based on the B3LYP geometries. For the barrierless association process, a limited number of constrained optimizations with a fixed interatomic C−N distance were carried out at the UB3LYP/6-311G(d,p) level. For each point along the path, the vibrational analysis (projecting out the imaginary frequency) was done. Considering the strong influence of electron correlation effects for the dissociation of a closed-shell molecule into a biradical, single-point energy calculations were done by the second-order multireference perturbation theory (CASPT2) with the aug-cc-pvtz basis set. Here, the active space was composed of 14 electrons in 10 orbitals, referred to as CASPT2(14,10). The CASPT2 calculations were carried out using the MOLPRO quantum chemistry package.[9]

The rate constants and product yields were calculated with the MultiWell program suite[10] based on VTST and RRKM statistical rate theory.[11−14] According to the RRKM theory, the energy-dependent unimolecular rate constant is written as $k(E) = (m^{\neq}/m)(\sigma_{ext}/\sigma_{ext}^{\neq})(g_e^{\neq}/g_e)(1/h)[G^{\neq}(E - E_0^T)]/[\rho(E)]$, where $m^{\neq}$ and m are the number of optical isomers, σ_{ext} and $\sigma_{ext}^{\neq}$ are the external rotation symmetry numbers, $g_e^{\neq}$ and g_e are the electronic state degeneracies of the transition state and reactant, respectively, h is Planck's constant, $G^{\neq}(E - E_0^T)$ is the sum of states of the transition state, $\rho(E)$ is the density of states of the reactant molecule, and E_0^T is the critical energy for reaction, including the zero-point energy (ZPE) and centrifugal corrections at temperature T. The details for the kinetics calculation will be given in the following discussions.

3. RESULTS AND DISCUSSION

The geometric parameters and the corresponding harmonic vibrational frequencies of the stationary points optimized at the B3LYP/6-311G(d,p) level are shown in Figure S1 and Table S1 (Supporting Information), respectively, along with the available experimental values for NO_2,[15−17] CH_2O,[15,18] NO,[16,19] HNO,[20−22] and H_2O.[16,21,23] It is shown that the optimized parameters agree well with the experimental data within a factor of 0.96−1.0, and the maximum deviation between theoretical and experimental frequencies is less than 7%.

3.1. Reaction Mechanism. The energy profile of the $CH_2Br + NO_2$ reaction calculated at the CCSD(T)/6-311++G(d,p)//B3LYP/6-311G(d,p) level is very similar to the previous result obtained at the CCSD(T)/6-311G(d,p)//B3LYP/6-311G(d,p) level by Pan et al.[5] For convenience of discussion, only the main reaction paths involved in the kinetic calculation are presented in Figure 1 in the text, and the whole PES information is shown in Figure S2 of the Supporting Information. On the singlet PES, the carbon-to-nitrogen approach is rather attractive to form CH_2BrNO_2 (**a**) without

dx.doi.org/10.1021/jp410811m | J. Phys. Chem. A 2014, 118, 3313−3318

any encounter barrier because both the C-terminus of CH_2Br and N-terminus of NO_2 have a single electron. The binding energy of **a** is −48.38 kcal/mol at the CCSD(T)/6-311++G(d,p)//B3LYP/6-311G(d,p) level, in good agreement with the result of Pan et al.[5] (−47.30 kcal/mol). Alternatively, the association process can proceed via the carbon-to-oxygen approach between CH_2Br and NO_2 at the O-site to form CH_2BrONO (**b1**). A considerable barrier (TSRb1) with the value of 2.11 kcal/mol is needed to activate the short N═O double bond (1.194 Å) in NO_2 to form the long N−O weak bond in **b1** (1.502 Å). TSRb1 has C_s symmetry, and the C−O bond is about 0.9 Å longer than its equilibrium structure **b1**. Clearly, the carbon-to-nitrogen entrance channel occurs more preferentially than the carbon-to-oxygen entrance channel.

Seen from Figure 1, isomer **a** (CH_2BrNO_2) can isomerize to the species **b1** (*trans*-CH_2BrONO) via TSab1 or **b2** (*cis*-CH_2BrONO) via TSab2. TSab1 lies about 7 kcal/mol above the reactants, while transition-state TSab2 is about 22.13 kcal/mol lower than the reactants. Thus, reaction pathway **a** → **b2** is the feasible pathway for the evolution of **a**. Starting from **b2**, there are two pathways to produce **P1** (BrNO + CH_2O), which is in agreement with the discussions of Pan et al.[5] Isomer **b2** dissociates directly via TSb2PRC to give postreaction complex **PRC**, which is 3.26 kcal/mol more stable than separate products **P1**. Also, **b2** can isomerize to **b1** via TSb1b2 and then dissociate to **PRC** via TSb1PRC to give product **P1**. The energies for TSb1b2 (−44.00 kcal/mol), TSb1PRC (−35.59 kcal/mol), and TSb2PRC (−34.60 kcal/mol) are very low, and the barriers for both channels are very close to each other; therefore, both dissociation pathways are favorable and competitive. **P1** can undergo direct dissociation to produce CH_2O + Br + NO **P2** due to the weakly bound N−Br bond. Because the energies of **P1** (−54.17 kcal/mol) and **P2** (−31.17 kcal/mol) are much lower than that of the reactant **R**, the formation of products CH_2O, BrNO, NO, and Br are all thermodynamically feasible. The formation pathways of **P1** and **P2** can be written as

Path 1:

$$\mathbf{R} \rightarrow CH_2BrNO_2\ \mathbf{a} \rightarrow CH_2BrONO\ \mathbf{b1}\ (\mathbf{b2})$$
$$\rightarrow CH_2O + BrNO\ \mathbf{P1} \rightarrow CH_2O + NO + Br\ \mathbf{P2}$$

Same as the previous results,[5] isomer **b1** can undergo a concerted H shift and O1−N rupture process (there are two transition states, i.e., TSb1P3 and TSb1P3-2) to produce CHOBr + HNO **P3**. However, they need to overcome a higher barrier than the formation of **P1**. Thus, these processes are less competitive than Path 1. Such processes can be written as

Path 2:

$$\mathbf{R} \rightarrow CH_2BrNO_2\ \mathbf{a} \rightarrow CH_2BrONO\ \mathbf{b1}\ (\mathbf{b2})$$
$$\rightarrow CHOBr + HNO\ \mathbf{P3}$$

In addition, there are other pathways that are energetically inaccessible due to the higher energies of their transition states. We will not discuss such processes. The detailed information can be found in Figure S2 of the Supporting Information.

As for the triplet PES of $CH_2Br + NO_2$, there are three entrance channels to produce triplet adducts ^{3}a (12.01 kcal/mol), ^{3}b1 (1.09 kcal/mol), and ^{3}b2 (3.81 kcal/mol). The relative energies of transition states for these entrance channels (^{3}TSRa, ^{3}TSRb1, and ^{3}TSRb2) are very high, with the values of 33.02, 21.27, and 22.42 kcal/mol, respectively. Therefore, the triplet pathways are unfavorable kinetically and will not be further discussed.

3.2. Calculations of the Rate Constants and Product Distribution. For the title reaction, the initial association process ($CH_2Br + NO_2 \rightarrow CH_2BrNO_2$ **a**) is barrierless, which is expected to be fast and plays an important role in the reaction kinetics, and the energy information in the barrierless entrance channel needs to be verified. However, the minimum-energy path (MEP) cannot be found from the IRC calculation for such a barrierless reaction. The accurate theoretical calculation of rate coefficients for this process would require the use of advanced methods such as variable reaction coordinate formulation of variational transition-state theory (VRC-VTST) coupled with multireference ab initio calculations.[24,25] This approach was not employed in this work, while an alternative method, that is, a distinguished coordinate path (DCP), was carried out for this association process because it is governed only by the interaction between the C atom of CH_2Br and the N atom of NO_2. The relaxed potential energy curve for the C−N separation of **a** from C−N distance r = 2.0 to 3.5 Å was obtained at the B3LYP/6-311G(d,p) level using tight convergence criteria. Subsequently, single-point energies at a high level are calculated using the CASPT2 method, and the total energies with ZPE correction at both levels are shown in Figure 2. Here, the zero of energy for the

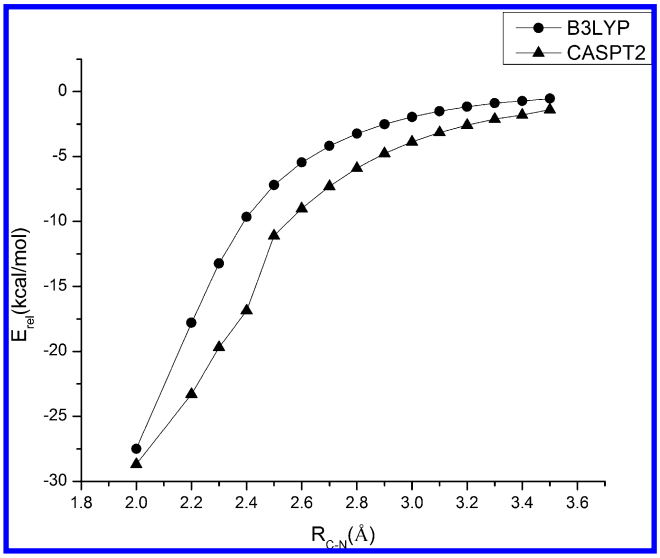

Figure 2. Relaxed scan of the C−N distance for isomer CH_2BrNO_2 (**a**) at the B3LYP/6-311G(d,p) and CASPT2(14,10)/aug-cc-pvtz//B3LYP/6-311G(d,p) levels. ZPEs are included.

CASPT2 method is taken to be the energy of the reactants at r = 20 Å. We can see from Figure 2 that adduct **a** is formed as the C atom of CH_2Br approaches the N atom of NO_2 without an intrinsic barrier, which is consistent with the previous assumption.[5] The energies calculated by the CASPT2 method will be used in the following kinetic calculation to determine the position of the loose transition state, so as to evaluate the VTST rate constants (see below).

Figure 3 shows the variation of the logarithm of vibrational harmonic frequencies for this approaching process, which will also be used in the subsequent rate constant calculations. During the calculation of frequencies, a project operator is used to remove the contribution of the gradient along the association

dx.doi.org/10.1021/jp410811m | J. Phys. Chem. A 2014, 118, 3313−3318

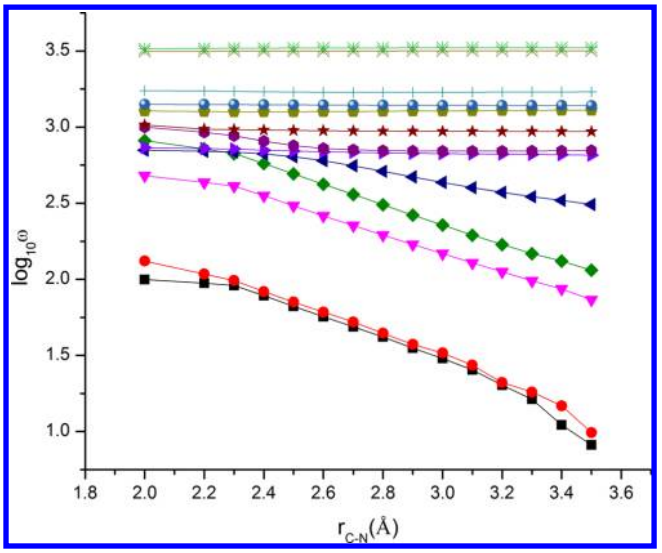

Figure 3. Vibrational frequencies calculated at the B3LYP/6-311G(d,p) level for different C−N bond distances r_{C-N}.

channel before performing a normal-mode analysis. Seen from Figure 3, eight of the normal-mode frequencies are almost constants, which correspond to the internal vibrational modes of the two reactants. In contrast, the other lowest six frequencies are decreasing as the C−N distance is increasing, which include the rotations of both reactants as well as the relative translational motions of them.

The overall rate constant for this recombination reaction can be computed according to the following expression

$$k(T) = (1 - f_R)k_{rec,\infty}(T) \quad (1)$$

where f_R is the fraction of redissociation of the initial adduct back to the initial reactant $CH_2Br + NO_2$ and $k_{rec,\infty}(T)$ is the high-pressure limit rate constant for the bimolecular recombination process, which is calculated as a function of temperature using VTST.[26−28] In the VTST calculations, rate constants have been performed at various points along the reaction coordinate for the initial association channel $CH_2Br + NO_2 \rightarrow$ **a**, and a search for the geometry yielded a minimum value of the rate constant. The lowest three points were used to find the final minimal rate constant using interpolation, with the quadratic functions ($f(r) = a \times r^2 + b \times r + c$, where a, b, and c are the fitted parameters and r is the distance).

In RRKM calculations, the Lennard-Jones parameters for bath gas He are $\sigma = 2.5$ and $\epsilon = 10$.[29] While those for **a**, **b1**, and **b2** ($\sigma = 4.85$ and $\epsilon = 606$) are obtained using the method of Stiel and Thodos,[30] which is suitable for very polar molecules, that is, $\sigma = 0.785V_c^{1/3}$ and $\epsilon = 0.897T_c$. Here, $V_c = 235.5$ cm^3/mol and $T_c = 675.81$ K are the critical volume and critical temperature, respectively, which are obtained by the Joback method.[31] For the title reaction, f_R values are very small and can be ignored in the measured temperature range, while they slightly increase as the temperature increases. For example, f_R is 0.112 at 2000 K. Once the intermediate **a** is formed, it will fall apart via isomerization and dissociation processes to produce products **P1** and **P3**. As a result, the calculated rate constants are pressure-independent, consistent with the experimental observation.[4]

The reaction rate constant for formation of the ith reaction product is given by $k_i(T) = f_i\, k_{rec,\infty}(T)$, where f_i is the fractional yield of the ith reaction product. The overall rate constants and individual rate constants for products (**P1** and **P3**) over the temperature range of 200−2000 K are shown in Figure 4 and

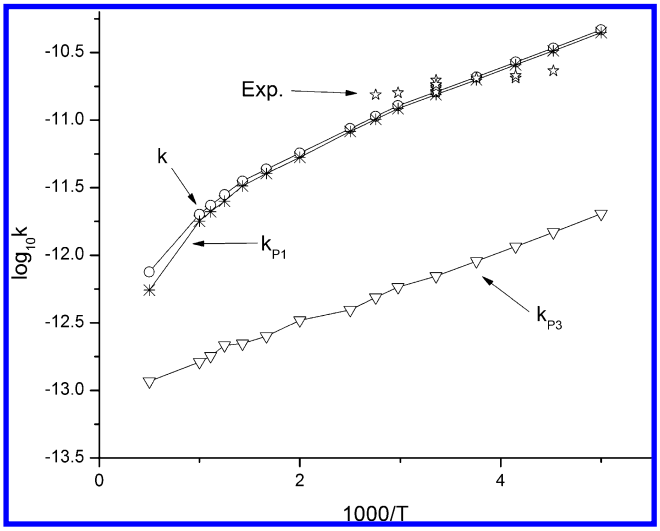

Figure 4. Calculated overall rate constant and individual rate constants for products, as well as the available experimental data.[4]

Table 1, as well as the available experimental data,[4] and branching ratios are shown in Figure 5. It is shown that the calculated rate constants are in good agreement with the experimental data, within the deviation of 0.69−1.47 in the measured temperature range. Negative temperature dependence of the rate constants is found below 2000 K, which is typical behavior for the radical−radical reaction, as confirmed experimentally.[4] The rate constants for product **P1** are about 1 or 2 orders of magnitude larger than those of product **P3**. As shown in Figure 5, the calculated ratios of **P1** are 96% at 200 K, 89% at 1000 K, and 73% at 2000 K, which indicate that CH_2O + BrNO (**P1**) is the dominant reaction route for the title reaction over the whole temperature range, in line with the experimental observation, while HNO + CHOBr (**P3**) may be produced with a minor contribution only at high temperatures.

The experimental data is lacking at other temperatures because the experiment was performed in a narrow temperature range for the title reaction. In order to offer further information concerning the reaction, the three-parameter fits based on the calculated rate constants at the CCSD(T)/6-311++G(d,p)//B3LYP/6-311G(d,p) level within 200−2000 K give the expression as follow (in units of cm^3 molecule^{-1} s^{-1}): $k(T) = 2.61 \times 10^{-10}T^{-0.76} \exp(461/T)$, $k_{P1}(T) = 4.64 \times 10^{-10}T^{-0.86} \exp(438/T)$, and $k_{P3}(T) = 4.09 \times 10^{-14}T^{0.11} \exp(662/T)$.

4. CONCLUSIONS

In the present work, the PES profile for the $CH_2Br + NO_2$ reaction was obtained at high level of theory CCSD(T)/6-311++G(d,p)//B3LYP/6-311G(d,p). On the singlet PES, the reaction is initiated by the carbon-to-nitrogen approach to barrierlessly form isomer CH_2BrNO_2 **a**, which is further verified by CASPT2(14,10)/aug-cc-pVTZ//B3LYP/6-311G(d,p) calculation for the entrance channel. Starting from **a**, three products **P1** (BrNO + CH_2O), **P2** (Br + NO + CH_2O), and **P3** (HNO + CHOBr) are predicted to be important. The contribution of the triplet pathways to the title reaction is negligible due to the high entrance barriers. Master equation simulations are employed to evaluate the distribution of primary products. Conventional RRKM product yields verify

Table 1. Rate Constants (k in 10^{-11} cm^3 molecule^{-1} s^{-1}) Obtained from the Master Equation Calculations and Available Experimental Data

T	k	exp.[a]
200	4.66	
221	3.41	2.32 ± 0.1
241	2.68	2.05 ± 0.13; 2.14 ± 0.03
266	2.09	2.05 ± 0.05
298	1.62	1.76 ± 0.08; 1.71 ± 0.06; 1.81 ± 0.06; 1.61 ± 0.03; 1.98 ± 0.08; 1.76 ± 0.03; 1.84 ± 0.03
336	1.28	1.59 ± 0.07
363	1.07	1.54 ± 0.04
400	0.865	
500	0.570	
600	0.433	
700	0.353	
800	0.281	
900	0.234	
1000	0.200	
2000	0.753	

[a]From ref 4.

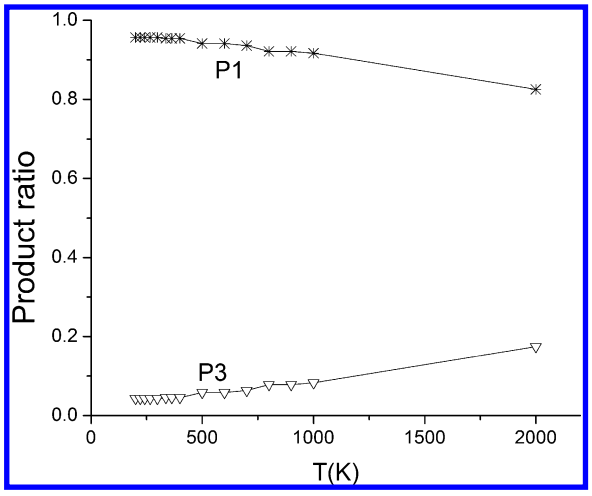

Figure 5. Calculated product ratios for products **P1** and **P3**.

the experimental findings that CH_2O is the main product and predict that **P3** may be produced with minor quantities in the reaction process. The calculated overall thermal rate constants agree well with the available experimental data in the measured temperature range. The overall rate constants as well as individual rate constants for products **P1** and **P3** are presented as $k(T) = 2.61 \times 10^{-10}T^{-0.76}\exp(461/T)$, $k_{P1}(T) = 4.64 \times 10^{-10}T^{-0.86}\exp(438/T)$, and $k_{P3}(T) = 4.09 \times 10^{-14}T^{0.11}\exp(662/T)$ cm^3 molecule^{-1} s^{-1} over the wide temperature range of 200−2000 K. This study is expected to provide valuable information for atmospheric chemistry and combustion chemistry.

■ ASSOCIATED CONTENT

Supporting Information

Schematic singlet potential energy surface of the relevant reaction pathways for the title reaction, as well as the optimized geometries and the corresponding frequencies. This material is available free of charge via the Internet at http://pubs.acs.org.

■ AUTHOR INFORMATION

Corresponding Author

*E-mail: ljy121@mail.jlu.edu.cn. Phone: 011-86-431-88498016.

Notes

The authors declare no competing financial interest.

■ ACKNOWLEDGMENTS

Correspondence with Jason A. Sonk is gratefully acknowledged.

J.-Y.L. acknowledges the National Nature Science Foundation of China (20973077, 21373098) and the Program for New Century Excellent Talents in University (NCET). J.R.B. acknowledges the National Science Foundation (Atmospheric and Geospace Sciences) and NASA (upper Atmospheric Research Program)

■ REFERENCES

(1) Miller, J. A.; Bowman, C. T. Mechanism and Modeling of Nitrogen Chemistry in Combustion. *Prog. Energy Combust. Sci.* **1989**, *15*, 287−338.

(2) Yung, Y. L.; Pinto, J. P.; Watson, R. T.; Sander, S. P. Atmospheric Bromine and Ozone Perturbations in the Lower Stratosphere. *J. Atmos. Sci.* **1980**, *37*, 339−353.

(3) Wenneberg, P. O.; Cohen, R. C.; Stimpfle, R. M.; Koplow, J. P.; Anderson, J. G.; Salawitch, R. J.; Fahey, D. W.; Woodbridge, E. L.; Keim, E. R.; Gao, R. S.; et al. Removal of Stratospheric O_3 by Radicals: In Situ Measurements of OH, HO_2, NO, NO_2, ClO, and BrO. *Science* **1994**, *266*, 398−404.

(4) Eskola, A. J.; Wojcik-Pastuszka, D.; Ratajczak, E.; Timonen, R. S. Kinetics of the Reactions of CH_2I, CH_2Br, and CHBrCl Radicals with NO_2 in the Temperature Range 220−360 K. *J. Phys. Chem. A* **2006**, *110*, 12177−12183.

(5) Jia, X.-J.; Pan, X.-M.; Sun, J.-Y.; Tang, Y.-Z.; Sun, H.; Pan, Y.-R.; Wang, R.-S. Theoretical Mechanistic Study on the Radical−Molecule Reaction of CH_2Br/CHBrCl with NO_2. *Theor. Chem. Acc.* **2009**, *122*, 207−216.

(6) Frisch, M. J.; Trucks, G. W.; Schlegel, H. B.; Scuseria, G. E.; Robb, M. A.; Cheeseman, J. R.; Montgomery, J. A., Jr.; Vreven, T.; Kudin, K. N.; Burant, J. C.; et al. *Gaussian03*, revision B.05; Gaussian, Inc.: Pittsburgh, PA. 2003.

(7) Becke, A. D. A New Mixing of Hartree−Fock and Local Density-Functional Theories. *J. Chem. Phys.* **1993**, *98*, 1372−1377.

(8) Lee, C.; Yang, W.; Parr, R. G. Development of the Colle−Salvetti Correlation-Energy Formula into a Functional of the Electron Density. *Phys. Rev. B* **1998**, *37*, 785−789.

(9) Werner, H.-J.; Knowles, P. J.; Knizia, G.; Manby, F. R.; Schütz, M.; Celani, P.; Korona, T.; Lindh, R.; Mitrushenkov, A.; Rauhut, G.; et al. *MOLPRO*, version 2010.1; 2010.

(10) *MultiWell-2013*, designed and maintained by John R. Barker with contributors Ortiz, N. F.; Preses, J. M.; Lohr, L. L.; Maranzana, A.; Stimac, P. J.; Nguyen, T. L.; Dhilip Kumar, T. J. University of Michigan: Ann Arbor, MI, 2013; http://aoss.engin.umich.edu/multiwell/.
(11) Robinson, P. J.; Holbrook, K. A. *Unimolecular Reactions*; Wiley-Interscience: New York, 1972.
(12) Forst, W. *Theory of Unimolecular Reactions*; Academic Press: New York, 1973.
(13) Gilbert, R. G.; Smith, S. C. *Theory of Unimolecular and Recombination Reactions*; Blackwell Scientific: Oxford, U.K., 1990.
(14) Baer, T.; Hase, W. L. *Unimolecular Reaction Dynamics. Theory and Experiments*; Oxford University Press: New York, 1996.
(15) Herzberg, G. *Electronic Spectra and Electronic Structure of Polyatomic Molecules*; Van Nostrand: New York, 1966.
(16) Shimanouchi, T. *Tables of Molecular Vibrational Frequencies*; Consolidated Volume *1*, Government Printing Office: Washington, D.C., 1972, NSRDS NBS-39.
(17) Sverdlov, L. M.; Kovner, M. A.; Krainov, E. P. *Vibrational Spectra of Polyatomic Molecules*; Wiley: New York, 1974.
(18) Nakanaga, T.; Kondo, S.; Saeki, S. Infrared Band Intensities of Formaldehyde and Formaldehyde-d_2. *J. Chem. Phys.* **1982**, *76*, 3860−3865.
(19) Huber, K. P.; Herzberg, G. *Molecular Spectra and Molecular Structure. IV. Constants of Diatomic Molecules*; Van Nostrand Reinhold Co: New York, 1979.
(20) Ogilvie, J. F. Structures of Triatomic Radicals HCO, HNO and HOO. *J. Mol. Struct.* **1976**, *31*, 407−401.
(21) Huber, K. P.; Herzberg, G. *Molecular Spectra and Molecular Structure. IV. Constants of Diatomic Molecules*; Van Nostrand Reinhold Co.: New York, 1979.
(22) Jacox, M. E. Vibrational and Electronic Energy Levels of Polyatomic Transient Molecules. *J. Phys. Chem. Ref. Data* **1994**, Monograph 3.
(23) Hoy, A. R.; Bunker, P. R. A Precise Solution of the Rotation Bending Schrödinger Equation for a Triatomic Molecule with Application to the Water Molecule. *J. Mol. Struct.* **1979**, *74*, 1−8.
(24) Miller, J. A.; Klippenstein, S. J.; Georgievskii, Y.; Harding, L. B.; Allen, W. D.; Simmonett, A. C. Reactions between Resonance-Stabilized Radicals: Propargyl + Allyl. *J. Phys. Chem. A* **2010**, *114*, 4881−4890.
(25) Georgievskii, Y.; Klippenstein, S. J. Transition State Theory for Multichannel Addition Reactions: Multifaceted Dividing Surfaces. *J. Phys. Chem. A* **2003**, *107*, 9776−9781.
(26) Forst, W. *Unimolecular Reaction. A Concise Introduction*; Cambridge University Press: Cambridge, U.K., 2003.
(27) Gilbert, R. G.; Smith, S. C. *Theory of Unimolecular and Rcombination Reaction*; Blackwell Scientific: Oxford, U.K., 1990.
(28) Holbrook, K. A.; Pilling, M. J.; Robertson, S. H. *Unimolecular Reaction*; Wiley: Chichester, U.K, 1996.
(29) Hippler, H.; Troe, J.; Wendelken, H. J. Collisional Deactivation of Vibrationally Highly Excited Polyatomic Molecules. II. Direct Observations for Excited Toluene. *J. Chem. Phys.* **1983**, *78*, 6709−6717.
(30) Stiel, L. I.; Thodos, G. Lennard-Jones Force Constants Predicted from Critical Properties. *J. Chem. Eng. Data* **1962**, *7*, 234−236.
(31) Joback, K. G.; Reid, R. C. Estimation of Pure-Component Properties from Group-Contributions. *Chem. Eng. Commun.* **1987**, *57*, 233−243.